How to cite: *Angew. Chem. Int. Ed.* **2022,** *61,* e202205701
International Edition: doi.org/10.1002/anie.202205701
German Edition: doi.org/10.1002/ange.202205701

Supramolecular Chemistry

Visible-Light-Responsive Self-Assembled Complexes: Improved Photoswitching Properties by Metal Ion Coordination**

*Ray G. DiNardi, Anna O. Douglas, Ruoming Tian, Jason R. Price, Mohammad Tajik, William A. Donald, and Jonathon E. Beves**

Abstract: A photoswitchable ligand based on azobenzene is self-assembled with palladium(II) ions to form a $[Pd_2(E\text{-}\mathbf{L})_4]^{4+}$ cage. Irradiation with 470 nm light results in the near-quantitative switching to a monomeric species $[Pd(Z\text{-}\mathbf{L})_2]^{2+}$, which can be reversed by irradiation with 405 nm light, or heat. The photoswitching selectivity towards the metastable isomer is significantly improved upon self-assembly, and the thermal half-life is extended from 40 days to 850 days, a promising approach for tuning photoswitching properties.

Introduction

Molecular assemblies that are addressable by non-destructive stimuli allow their properties to be adjusted at will. Visible light is an ideal stimulus that can be applied with high-resolution in time and space and, in principle, can be used without any buildup of chemical waste. One of the most appealing ways to introduce reversible light-responsive behavior to synthetic systems is by including molecular photoswitches.[1] Azobenzene[2] and related compounds have been widely used to develop responsive receptors,[3] light responsive containers,[4] metal complexes with switchable magnetic properties,[5] photopharmacology,[6] polymers,[7] metal–organic frameworks,[8] and other types of assembled materials[9,10] including gels.[11] The binding of the different azobenzene isomers in macrocycles[12] has also allowed the formation of networks, including an especially impressive example where such interactions control the assembly of macroscale gel pieces.[13]

While there are many examples of photoswitchable receptors,[14] there are relatively few examples of discrete assemblies that can be switched with visible light. Photoswitchable groups have been appended on the exterior[15] or interior[16] of assemblies that are self-assembled with metal ions,[17,18] rather than the photoswitch acting as a structural element. This is due to, in part, that metal ion coordination[19] can limit photoswitching, especially for photoswitches that undergo significant geometry changes.[20] For example, when an azobenzene-appended ligand was self-assembled into a molecular sphere with palladium(II) ions, the azobenzene units could only be isomerized to form 17 % of the metastable *Z*-isomer, compared to 65 % in the free ligand.[16] In another example, azobenzene ligands were assembled with palladium(II) to give a cage reported to isomerize to 69 % of the *Z*-isomer.[21] Macrocycles functionalized with azobenzenes have been self-assembled with hydrogen bonds to form dimeric[22] or hexameric capsules[23] where around 60–70 % of the azobenzenes can be isomerized when irradiated.

Using the self-assembly approach pioneered by McMorran and Steel,[24] the Clever group have developed a series of M_2L_4 molecular cages with dithienylethene (DTE) photoswitches[25] that can be isomerized near-quantitatively between open and closed forms with light. This switching causes a shape change of the cage to result in impressive changes to guest binding properties. The cages are mixtures of diastereoisomers as the closed isomer of the DTE photoswitch is chiral, which was later exploited using chiral guests to amplify the chirality of the cage.[25a] Crowded alkene switches with pendant pyridyl groups have also been self-assembled into homochiral Pd_2L_4 molecular cages that could be switched with UV light.[26]

Azobenzene has been included as a structural element[21,27] in metal-templated self-assembled structures, with an early macrocycle examples by Lees[27a] and the first cage example reported by Hardie.[27b] In Hardie's example, photoswitchable groups could be isomerized up to 40 % in the cage, while the topology of the structure was maintained during switching. Cages formed by bridged azobenzenes (diazocines) and palladium(II) ions can be isomerized to around 65 % of the metastable isomer using visible light, essentially identical to the behavior of the free ligand.[28]

[*] R. G. DiNardi, A. O. Douglas, Dr. J. R. Price, M. Tajik, Prof. W. A. Donald, Prof. J. E. Beves
School of Chemistry, UNSW Sydney
Sydney, NSW 2052 (Australia)
E-mail: j.beves@unsw.edu.au
Dr. R. Tian
Crystallography laboratory, Mark Wainwright Analytical Centre, UNSW Sydney
Sydney, NSW 2052 (Australia)
Dr. J. R. Price
ANSTO, The Australian Synchrotron
800 Blackburn Rd, Clayton, Vic 3168 (Australia)

[**] A previous version of this manuscript has been deposited on a preprint server (https://doi.org/10.26434/chemrxiv-2022-g5f6k-v4).

We recently reported the first example of self-assembled cages that were switchable with visible light.[29] *ortho*-Tetrafluoroazobenzene[30,31]-based ligands with appended pyridyl groups were assembled with palladium(II) ions to form a dynamic mixture of two species (trimer and tetramer). In that case, the most thermodynamically stable species could be selectively disassembled using light by isomerizing just 15 % to the metastable isomer.[29] Herein, we report a new photoswitchable ligand that can be assembled into a single well-defined cage structure and reversibly switched to another discrete structure using visible light (Figure 1).

Results and Discussion

The photoswitchable ligand **1** was synthesized from readily available 4-bromo-2,6-difluoroaniline following a modified literature procedure,[29,30] see Supporting Information S2 for details. The ligand was characterized using ^{1}H, ^{19}F and ^{13}C NMR spectroscopy (Supporting Information S2), UV/Vis absorption spectroscopy (Figure 2, Supporting Information S3), and mass spectrometry (see Supporting Information S6). A single crystal suitable for X-ray diffraction was grown by the slow evaporation of a solution of *E*-**1** in $CH_3CN/CHCl_3$/toluene. The solid state structure of *E*-**1** (Figure 3a) is flat with the phenyl rings perfectly coplanar,[32] unlike in the structure of the parent *ortho*-tetrafluoroazobenzene.[31n]

We studied the photoswitching behavior of **1** in DMSO using NMR and UV/Vis spectroscopy techniques (see Supporting Information S3 for details). We started by determining the photostationary state (PSS) distributions of the thermodynamically stable *E*-isomer and metastable *Z*-isomer using different irradiation wavelengths (Figure 2). Violet light centered at 405 nm provided the best selectivity towards *E*-**1** (80 % *E*), while red light centered at 617 nm provided the best selectivity towards *Z*-**1** (90 % *Z*). A 1:1 mixture of *E*-**1** and *Z*-**1** is generated by irradiating with blue light centered at 470 nm. When violet or blue light are used a PSS is rapidly reached, whereas a red-light source took ≈2 hours to reach a PSS. Green light centered at 530 nm offers reasonable selectivity towards *Z*-**1** (80 % *Z*), while also generating a PSS within 5 min. Photoswitch **1** has poorer photo-selectivity compared to the parent *ortho*-tetrafluoroazobenzene[30b] resulting from smaller separation

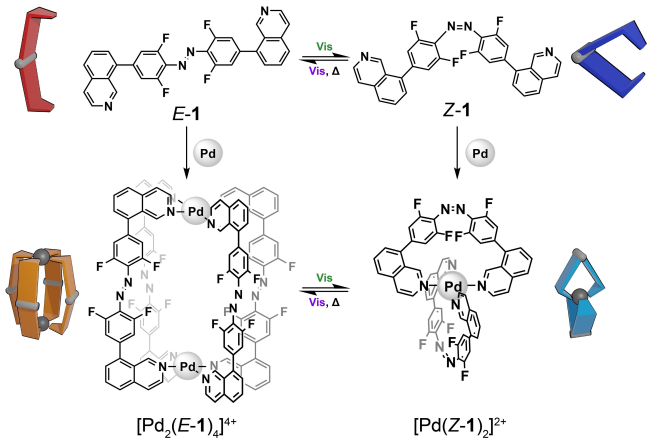

Figure 1. Visible-light responsive photoswitchable ligand **1** and self-assembled products $[Pd_2(E\text{-}\mathbf{1})_4]^{4+}$ and $[Pd(Z\text{-}\mathbf{1})_2]^{2+}$.

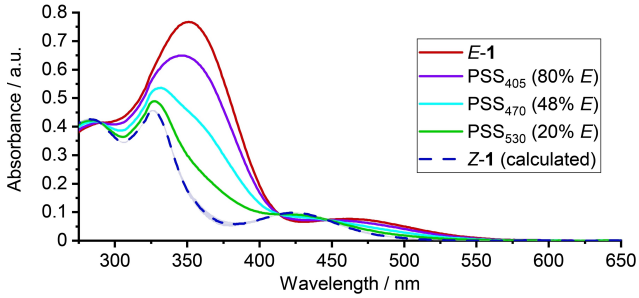

Figure 2. The UV/Visible absorption (DMSO, 298 K) spectra of photoswitch **1** at PSS generated using LEDs with emission centered at various wavelengths. The spectrum for *Z*-**1** was calculated using the ^{1}H and ^{19}F NMR data together with absorption spectra solutions at PSS when irradiated with 405, 470, 530 and 617 nm. See Supporting Information S3 for details.

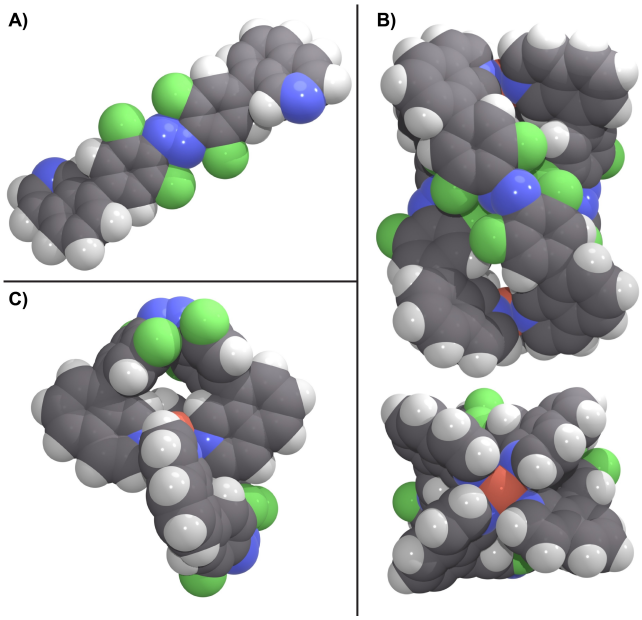

Figure 3. a) Single crystal X-ray structures of *E*-**1**.[32] The N=N bond length is 1.243(2) Å and C_{Ar}–N is 1.414(2) Å. The asymmetric unit contains half the molecule and the two phenyl rings are perfectly coplanar, with C–N=N bond angles of 115.24°, and C(F)–C–N=N torsion angle of 177.6(1)°. The parent *ortho*-tetrafluoroazobenzene[31n] is less planar, with C(F)–C–N=N torsion angles of 139.29 and 139.41°. b) Major positional conformer of $[Pd_2(E\text{-}\mathbf{1})_4]^{4+}$ in the single crystal X-ray structure of $[Pd_2(E\text{-}\mathbf{1})_4](BF_4)_4 \cdot 0.5H_2O \cdot 4CH_3CN$.[32] The ligands adopt a range of conformations, with one ligand almost planar and others twisted with the two phenyl rings demonstrating no clear conformational preference in the solid state. c) Major positional disorder of $[Pd(Z\text{-}\mathbf{1})_2]^{2+}$ in the single crystal X-ray structure of $[Pd(Z\text{-}\mathbf{1})_2](BF_4)_2 \cdot 2CH_3CN \cdot 0.8$ (MePh).[32] For crystallography details, see Supporting Information S11.

of the n-π* absorption bands of the two isomers, an observation that is in line with previous reports.[29,30b] The stable *E*-isomer can be fully recovered using heat, with *Z*-**1** having a 298 K thermal isomerization barrier of 111 kJ mol^{-1}, corresponding to half-life of ≈40 days (measured by variable temperature NMR, see Supporting Information S3.3).

To prepare photoswitchable self-assembled structures, two equivalents of photoswitchable ligand **1** were reacted with one equivalent of $[Pd(CH_3CN)_4](BF_4)_2$ in DMSO-d_6 (Supporting Information S4). The UV/Vis absorption spectrum in DMSO is very similar to that of *E*-**1** (Supporting Information S7). The ^{1}H and ^{19}F NMR spectra indicates the self-assembly of a symmetric single major species over 2 hours at room temperature (Figure 4A ii). Electrospray ionization mass spectrometry (ESI-MS) identified a $[Pd_2(\mathbf{1})_4]^{4+}$ composition (Figure 4B, Supporting Information S6) and NMR diffusion experiments show the structure has a 23 Å diameter (Supporting Information S5).

A single crystal suitable for X-ray diffraction was grown by slowly diffusing of a solution of $[Pd_2(E\text{-}\mathbf{1})_4]^{4+}$ in CH_3CN/$CHCl_3$ into toluene. The helical structure of $[Pd_2(E\text{-}\mathbf{1})_4]^{4+}$ is shown in Figure 3b.[32] Both palladium(II) centers are square planar as expected. Three of the four ligands have whole-ligand disorder with each adopting two major conformations. It is clear some pedal motion[33] is occurring in the solid without significant change to the volume or shape of the overall assembly.

Observing the pedaling motion demonstrates the flexible nature of the self-assembled cage. In solution the ^{1}H, ^{19}F and ^{13}C NMR spectra are consistent with fast rotation of the phenyl rings, and/or of fast twisting of the helical structure from one helicity to the other. Such helicity inversion can occur without breaking any bonds and would change the cavity size and shape significantly, similar to the ability of flexible cages to accommodate guests by adjusting their cavity size.[34] In the solid state the central cavity accommodates acetonitrile solvent molecules, demonstrating capacity for guest binding.

When $[Pd_2(E\text{-}\mathbf{1})_4](BF_4)_4$ is irradiated with green light centered at 530 nm a new major species is formed (Figure 4A iii). ESI-MS (Figure 4B, Supporting Information S6) and diffusion NMR experiments indicate that this new species composes $[Pd(\mathbf{1})_2]^{2+}$ and has hydrodynamic diameter of 16 Å. This demonstrated that visible light can be used to cleanly convert $[Pd_2(E\text{-}\mathbf{1})_4]^{4+}$ to $[Pd(Z\text{-}\mathbf{1})_2]^{2+}$. The synthesis of $[Pd_2(E\text{-}\mathbf{1})_4]^{4+}$ and $[Pd(Z\text{-}\mathbf{1})_2]^{2+}$ is concentration dependent. By diluting a 1:1 mixture of $[Pd_2(E\text{-}\mathbf{1})_4]^{4+}$ and $[Pd(Z\text{-}\mathbf{1})_2]^{2+}$ ([**1**] = 2.1 mM to [**1**] = 0.4 mM], DMSO, 298 K), ^{1}H NMR spectroscopy revealed the disassembly of the self-assembled products and the formation uncoordinated ligand **1** (See Supporting Information S4.2 for details). Single crystals of $[Pd(Z\text{-}\mathbf{1})_2]^{2+}$ were grown by slowly diffusing a solution of $[Pd(Z\text{-}\mathbf{1})_2]^{2+}$ in CH_3CN/CH_2Cl_2 into toluene. The crystals were used to determine the structure of $[Pd(Z\text{-}\mathbf{1})_2]^{2+}$ [32] as shown in Figure 3c. The complex has one ordered ligand and one whole-ligand disorder, and confirms the *trans*-configuration of the ligand coordination to the palladium(II) center. The structure shows how the ligands encapsulate the palladium(II) ion, limiting access above and below the square-planar geometry which would be required for ligand exchange to occur. Heating a sample of $[Pd(Z\text{-}\mathbf{1})_2]^{2+}$ in DMSO (363 K, 16 h) regenerated $[Pd_2(E\text{-}\mathbf{1})_4]^{4+}$ (Figure 4A iv).

The clean conversion of $[Pd_2(E\text{-}\mathbf{1})_4]^{4+}$ to $[Pd(Z\text{-}\mathbf{1})_2]^{2+}$ led us to investigate how the PSS distributions of photoswitch **1** are affected after the addition of palladium(II). We generated a 1:1 (48:52) mixture of *E*-**1** and *Z*-**1** (two equiv.)

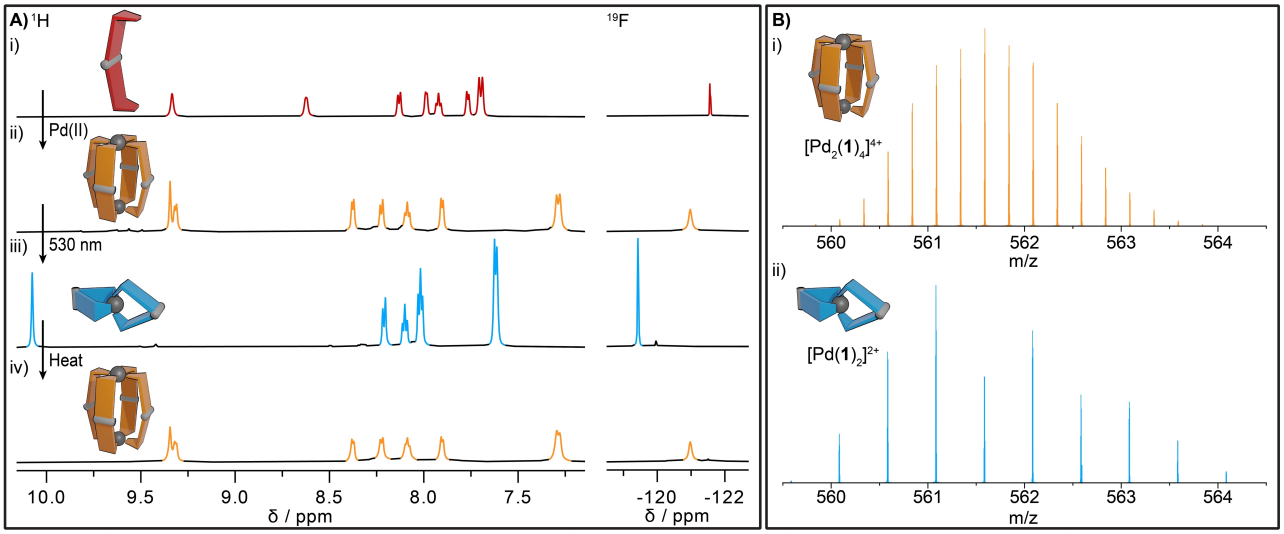

Figure 4. A) Partial ^{1}H (DMSO-d_6, 600 MHz, 298 K) and ^{19}F (DMSO-d_6, 565 MHz, 298 K) NMR spectra of i) photoswitch *E*-**1** ([**1**] = 10 mM, 2 equiv.); ii) the same sample after adding $[Pd(CH_3CN)_4](BF_4)_2$ (5.2 mM, 1 equiv.), iii) the same sample immediately after irradiating with 530 nm light for 15 min, and iv) the same sample after heating in the dark for 16 h at 90 °C and equilibrating at room temperature for 30 min. B) Zoom scans of select high resolution ESI-MS peaks for a sample of i) $[Pd_2(E\text{-}\mathbf{1})_4](BF_4)_4$ ([**1**] = 16 mM), corresponding to $[Pd_2(\mathbf{1})_4]^{4+}$, and ii) the same sample after irradiating with 530 nm light for 20 min, corresponding to $[Pd(\mathbf{1})_2]^{2+}$. See Supporting Information S6 for more details.

using blue light centered at 470 nm (Figure 5i) and added $[Pd(CH_3CN)_4](BF_4)_2$ (one equiv.) in DMSO-d_6. The ^{1}H and ^{19}F NMR spectra showed the rapid formation of complex $[Pd(Z\text{-}\mathbf{1})_2]^{2+}$ within 5 minutes, followed by the slower formation of cage $[Pd_2(E\text{-}\mathbf{1})_4]^{4+}$ over 2 hours (Figure 5ii). Irradiating this sample with light centered at either 470 nm (Figure 5iii) or 530 nm (Figure 5v) causes the near-quantitative conversion to $[Pd(Z\text{-}\mathbf{1})_2]^{2+}$. To ensure the photoswitching is still reversible in the presence of palladium(II), we cycled through irradiating a sample with light centered at 405 nm and 530 nm (Figure 5iv, v) to switch between mixtures of $[Pd_2(E\text{-}\mathbf{1})_4]^{4+}$ and $[Pd(Z\text{-}\mathbf{1})_2]^{2+}$, see Supporting Information S8 for details. As another control experiment, three separate samples of cage $[Pd_2(E\text{-}\mathbf{1})_4]^{4+}$ were irradiated with light centered at either 405 nm, 470 nm, or 530 nm. Excess 4-dimethylaminopyridine (DMAP) in DMSO-d_6 was added to each sample to form $[Pd(DMAP)_4]^{2+}$ and release the free ligand,[35] allowing the relative abundance of *E*-**1** and *Z*-**1** to be determined using ^{1}H NMR spectroscopy (Table 1). The sample irradiated with 470 nm light generated 95 % $[Pd(Z\text{-}\mathbf{1})_2]^{2+}$, and after adding DMAP the free ligand was 89 % *Z*-**1**.[36] In contrast, irradiating photoswitch **1** with the same light produces a PSS comprising just 52 % *Z*-**1**, demonstrating unambiguously that metal ion coordination significantly improves the PSS selectivity towards the metastable isomer.

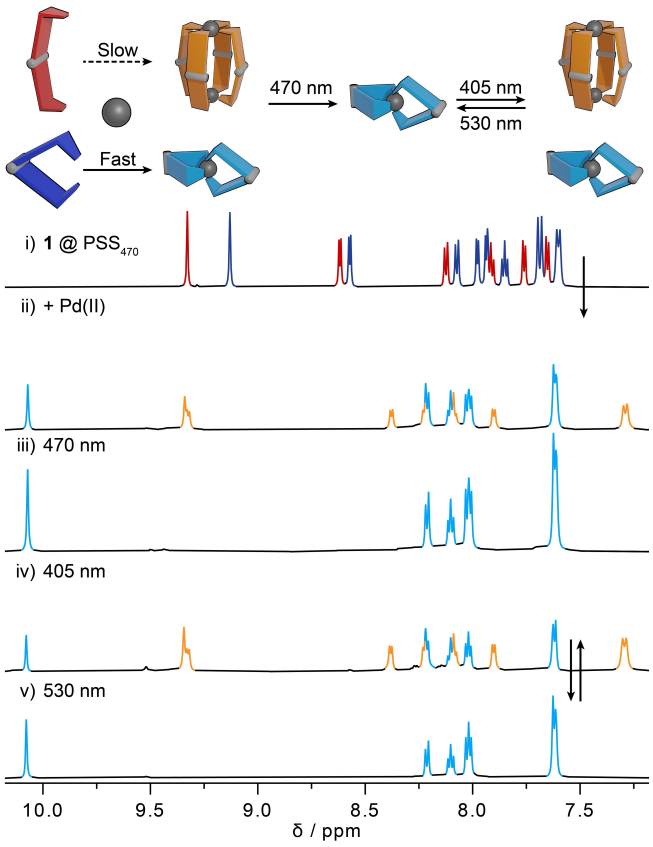

Figure 5. Partial ^{1}H NMR (DMSO-d_6, 600 MHz, 298 K) spectra of i) A 1:1 mixture of *E*-**1** and *Z*-**1** generated using 470 nm light ([**1**] = 1.6 mM, 2 equiv.), ii) the same sample 2 hours after adding $[Pd(CH_3CN)_4](BF_4)_2$ (0.82 mM, 1 equiv.), and iii) the same sample after irradiating with 470 nm light for 20 min, see Supporting Information S8 for details. iv) a mixture of $[Pd_2(E\text{-}\mathbf{1})_4](BF_4)_4$ and $[Pd(Z\text{-}\mathbf{1})_2](BF_4)_2$ ([**1**] = 7.1 mM) after irradiating with 405 nm light for 20 min, and v) the sample after irradiating with 530 nm light for 20 min, for more details see Supporting Information S8.

Table 1: Photostationary state distributions for photoswitchable ligand **1** with and without added palladium.[a]

Entry	PSS 405 nm % *Z*-**1**	PSS 470 nm % *Z*-**1**	PSS 530 nm % *Z*-**1**
1	20	52	80
1 + Pd^{II}[b]	54	95	> 98
1 + Pd^{II} + DMAP[c]	50	89	96

[a] Measured by ^{1}H (600 MHz, DMSO-d_6, 298 K) and ^{19}F NMR (565 MHz, DMSO-d_6, 298 K) data. [b] NMR spectra collected immediately after being irradiated for 30 min. [c] Immediately after the addition of ≈50 equiv. of DMAP. See Supporting Information S8 for details.

We considered the possibility of the ligands only isomerizing when dissociated from the palladium ion. If this were the case then an identical PSS should be reached whether palladium is present or not, provided the complexes do not significantly alter the spectrum of light available to the free ligands. To test this idea, a 1:1 mixture (46:54) sample of *E*-**1**:*Z*-**1** (four equiv.) was prepared by irradiating **1** with 470 nm light, then $[Pd(CH_3CN)_4](BF_4)_2$ (one equiv.) was added. This results in the rapid formation of $[Pd(Z\text{-}\mathbf{1})_2]^{2+}$ and the slower formation of $[Pd_2(E\text{-}\mathbf{1})_4]^{4+}$ over 12 h to give a 1:1 (51:49) ratio of the two complexes (in terms of the ligand concentration), and leaving free *E*-**1**:*Z*-**1** in 39:61 ratio (Supporting Information S8.4). This demonstrates the minor preference for the formation of palladium(II) complexes with the *E*-**1** over *Z*-**1**. The sample was then irradiated with 470 nm light until a PSS was reached (20 min). The distribution of the free ligand *E*-**1**:*Z*-**1** (45:55) at this PSS is the same as that for the free ligand in solution without added palladium (46:54). No $[Pd_2(E\text{-}\mathbf{1})_4]^{4+}$ was observed at the PSS, with the only complex being $[Pd(Z\text{-}\mathbf{1})_2]^{2+}$. This indicates that the photoswitching behavior of the free ligand is unchanged by the presence of the complexes and that the change in switching properties occurs either because switching can occur upon the coordinated ligands, or that the kinetics of ligand exchange of the two complexes is significantly different.

The next significant difference in switching behavior was the slower thermal isomerization from $Z \rightarrow E$ in the presence of palladium(II). A sample of $[Pd(Z\text{-}\mathbf{1})_2]^{2+}$ was heated at 363 K and monitored by ^{1}H NMR spectroscopy, (Figure 6). At 363 K, $[Pd(Z\text{-}\mathbf{1})_2]^{2+}$ had a thermal half-life of 192 min, whereas *Z*-**1** alone had a half-life of 33 min. These correspond to room temperature (298 K) thermal half-lives of 850 days for $[Pd(Z\text{-}\mathbf{1})_2]^{2+}$ and only 40 days for free *Z*-**1**. When a sample of $[Pd(Z\text{-}\mathbf{1})_2]^{2+}$ was diluted, the thermal half-life was shorter, consistent with the proportion of free ligand increasing which can isomerize much faster than when it is coordinated (see Supporting Information S9 for details). The thermal relaxation from $[Pd(Z\text{-}\mathbf{1})_2]^{2+}$ to $[Pd_2(E\text{-}\mathbf{1})_4]^{4+}$ does not follow first-order kinetics, which is

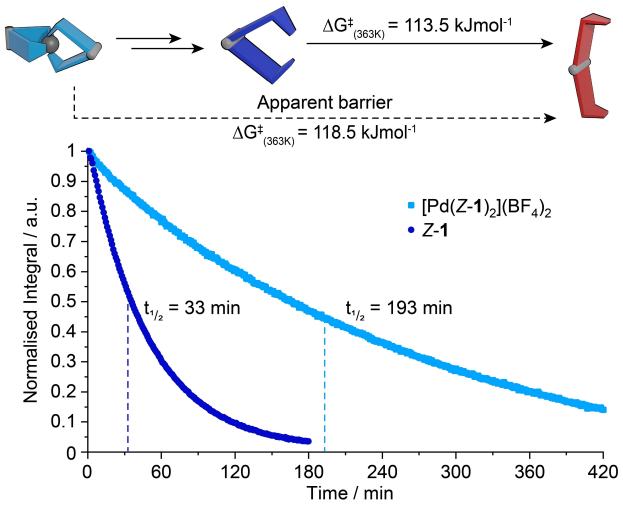

Figure 6. Comparison of thermal isomerization of *Z*-**1** ([**1**] = 8.7 mM) and $[Pd(Z\text{-}\mathbf{1})_2](BF_4)_2$ ([**1**] = 7.9 mM), using ^{1}H NMR (500 MHz, DMSO-d_6, 363 K) integrals of photoswitch *Z*-**1** (9.14 ppm) and $[Pd(Z\text{-}\mathbf{1})_2](BF_4)_2$ (10.07 ppm) normalized to initial integrals. The barrier for the thermal isomerization of *Z*-**1** at 363 K was measured at variable temperature (see Supporting Information S3.3 for details). The apparent barrier for the relaxation of $[Pd(Z\text{-}\mathbf{1})_2](BF_4)_2$ was determined by monitoring its depletion at 363 K.

unsurprising given the mechanistic complexity of the process (see Supporting Information S9).

Most commonly, photoswitchable receptors are used to switch binding properties, rather than the binding properties being used to control photoswitching properties.[14a,b,37] However, there are well known examples where intermolecular interactions do change photoswitching properties such as Shinkai's classic azobenzene-linked crown ethers that can drive the PSS to 98 % *Z* when Rb^I is bound,[38] and Rebek's azobenzene-containing receptor where the PSS modestly depends on the guest bound (from *E* 62 % to 40–72 % with guests).[39] An anion receptor also increased the rate of thermal *Z*→*E* isomerization when guests were bound.[40] The *Z*-isomer of an azobenzene-bridged bis-terpyridine ligand forms a mononuclear complex with iron(II) ions which extended the thermal stability of the *Z*-isomer by a factor of 2000, but coordination also prevents the photoswitching properties of ligand.[20b] The protonation of azobenzenes can significantly change their absorption and switching properties, such as the tetra-*ortho*-methoxy substituted azobenzenes[41] or azobenzazoles.[42] Protonation can also accelerate the Z→E thermal isomerization.[43] Hydrogen-bonded complexes have also been shown to accelerate *Z*→*E* isomerization,[44] while in other cases aggregation has slowed the *Z*→*E* isomerization time by two orders of magnitude.[45] Despite these examples, to the best of our knowledge the work here is the first where the rate of *Z*→*E* isomerization is decreased by coordination to transition metal ions and where the ligand retains its photoswitching properties. As such it offers a new method for controlling the photoswitching properties of azobenzenes.

We measured the binding affinities of $[Pd_2(E\text{-}\mathbf{1})_4](BF_4)_4$ and $[Pd(Z\text{-}\mathbf{1})_2](BF_4)_2$ for sulfonate guests in DMSO-d_6 by ^{1}H NMR titrations. These anionic guests were selected because neutral guests are often outcompeted by ions,[46] and these types of arylsulfonates have been shown to be good binders inside related Pd_2L_4 cages.[47] Addition of the disodium salt of 2,6-naphthalenedisulfonate to $[Pd_2(E\text{-}\mathbf{1})_4]^{4+}$ (1.1 mM) or $[Pd(Z\text{-}\mathbf{1})_2]^{2+}$ (2.2 mM) resulted in mixtures of species and uncoordinated ligand **1** as well as the formation of a precipitate (see Supporting Information 10.1 for details). Similar behavior has been reported for a related complex with the same anion.[28] Using tetrabutylammonium *p*-toluenesulfonate as a guest, we determined the 1:2 (H:G) non-cooperative binding constant for $[Pd_2(E\text{-}\mathbf{1})_4](BF_4)_2$ (1.2 mM, DMSO, 298 K), as 76 M^{-1} (see Supporting Information for details, SI-10.2).[48] The ^{1}H NMR signal that shifted the most corresponds to that of the proton adjacent to the quinoline nitrogen, outside the cavity ($\Delta\delta$ = +0.11 ppm). This indicates that the guest is associated with the palladium on the outside of the cage, rather than being encapsulated. A similar NMR titration was performed with *p*-toluenesulfonate and $[Pd(Z\text{-}\mathbf{1})_2](BF_4)_2$ (2.4 mM) to find a 1:1 binding constant of 17 M^{-1}, approximately 4-fold weaker than the binding affinity of $[Pd_2(E\text{-}\mathbf{1})_4](BF_4)_4$ (76 M^{-1}) for the same guest under the same conditions. Given reported examples of catalysis by $[Pd_2L_4]^{4+}$ cages,[49] this type of switchable binding has the potential to control the catalytic activity of such assemblies using visible light.

Conclusion

We have shown how coordination of a molecular photoswitch to palladium(II) ions both increased the kinetic stability of the metastable *Z*-isomer, and significantly improved the photostationary state distribution. The resulting complexes have different properties—size, shape and reactivity—allowing visible light and heat to reversibly switch between two discrete self-assembled structures.

Acknowledgements

This work was supported by the Australian Research Council (FT170100094). We acknowledge the Mark Wainwright Analytical Centre at UNSW Sydney for access to the NMR, X-ray diffraction and mass spectrometry facilities. Open access publishing facilitated by University of New South Wales, as part of the Wiley - University of New South Wales agreement via the Council of Australian University Librarians.

Conflict of Interest

The authors declare no conflict of interest.

Data Availability Statement

The data that support the findings of this study are openly available in ChemRxiv at https://doi.org/10.26434/chemrxiv-2022-g5f6k, reference number 1.

Keywords: Metal-Template · Molecular Cage · Non-Equilibrium · Photoswitch · Self-Assembly

[1] Z. L. Pianowski, *Chem. Eur. J.* **2019**, *25*, 5128–5144.

[2] F. A. Jerca, V. V. Jerca, R. Hoogenboom, *Nat. Chem. Rev.* **2022**, *6*, 51–69.

[3] G. Moncelsi, P. Ballester, *ChemPhotoChem* **2019**, *3*, 304–317.

[4] A. Díaz-Moscoso, P. Ballester, *Chem. Commun.* **2017**, *53*, 4635–4652.

[5] a) S. Venkataramani, U. Jana, M. Dommaschk, F. D. Sönnichsen, F. Tuczek, R. Herges, *Science* **2011**, *331*, 445–448; b) S. Shankar, M. Peters, K. Steinborn, B. Krahwinkel, F. D. Sönnichsen, D. Grote, W. Sander, T. Lohmiller, O. Rüdiger, R. Herges, *Nat. Commun.* **2018**, *9*, 4750; c) V. Wellm, C. Näther, R. Herges, *J. Org. Chem.* **2021**, *86*, 9503–9514.

[6] a) W. A. Velema, W. Szymanski, B. L. Feringa, *J. Am. Chem. Soc.* **2014**, *136*, 2178–2191; b) I. M. Welleman, M. W. H. Hoorens, B. L. Feringa, H. H. Boersma, W. Szymański, *Chem. Sci.* **2020**, *11*, 11672–11691.

[7] a) G. S. Kumar, D. C. Neckers, *Chem. Rev.* **1989**, *89*, 1915–1925; b) P. Weis, S. Wu, *Macromol. Rapid Commun.* **2018**, *39*, 1700220; c) J. Vapaavuori, C. G. Bazuin, A. Priimagi, *J. Mater. Chem. C* **2018**, *6*, 2168–2188.

[8] O. S. Bushuyev, T. Friščić, C. J. Barrett, *CrystEngComm* **2016**, *18*, 7204–7211.

[9] a) S. Yagai, T. Karatsu, A. Kitamura, *Chem. Eur. J.* **2005**, *11*, 4054–4063; b) W.-C. Xu, S. Sun, S. Wu, *Angew. Chem. Int. Ed.* **2019**, *58*, 9712–9740; *Angew. Chem.* **2019**, *131*, 9814–9843; c) P. Tecilla, D. Bonifazi, *ChemistryOpen* **2020**, *9*, 538–553; d) A. Goulet-Hanssens, F. Eisenreich, S. Hecht, *Adv. Mater.* **2020**, *32*, 1905966; e) S. Chen, R. Costil, F. K.-C. Leung, B. L. Feringa, *Angew. Chem. Int. Ed.* **2021**, *60*, 11604–11627; *Angew. Chem.* **2021**, *133*, 11708–11731.

[10] For example, azobenzene derivatives capable of hydrogen bonding interactions can be switched from the thermodynamically stable *E* isomer to the metastable *Z* isomer to change from a linear polymer to a discrete tetramer. a) F. Rakotondradany, M. A. Whitehead, A.-M. Lebuis, H. F. Sleiman, *Chem. Eur. J.* **2003**, *9*, 4771–4780.

[11] C. Wang, K. Hashimoto, R. Tamate, H. Kokubo, M. Watanabe, *Angew. Chem. Int. Ed.* **2018**, *57*, 227–230; *Angew. Chem.* **2018**, *130*, 233–236.

[12] J. del Barrio, P. N. Horton, D. Lairez, G. O. Lloyd, C. Toprakcioglu, O. A. Scherman, *J. Am. Chem. Soc.* **2013**, *135*, 11760–11763.

[13] H. Yamaguchi, Y. Kobayashi, R. Kobayashi, Y. Takashima, A. Hashidzume, A. Harada, *Nat. Commun.* **2012**, *3*, 603.

[14] For examples of photoswitchable receptors, see a) S. Wiedbrauk, T. Bartelmann, S. Thumser, P. Mayer, H. Dube, *Nat. Commun.* **2018**, *9*, 1456; b) X. Chi, W. Cen, J. A. Queenan, L. Long, V. M. Lynch, N. M. Khashab, J. L. Sessler, *J. Am. Chem. Soc.* **2019**, *141*, 6468–6472; c) T. S. C. MacDonald, B. L. Feringa, W. S. Price, S. J. Wezenberg, J. E. Beves, *J. Am. Chem. Soc.* **2020**, *142*, 20014–20020; d) S. J. Wezenberg, L.-J. Chen, J. E. Bos, B. L. Feringa, E. N. W. Howe, X. Wu, M. A. Siegler, P. A. Gale, *J. Am. Chem. Soc.* **2022**, *144*, 331–338.

[15] Y. Qin, L.-J. Chen, Y. Zhang, Y.-X. Hu, W.-L. Jiang, G.-Q. Yin, H. Tan, X. Li, L. Xu, H.-B. Yang, *Chem. Commun.* **2019**, *55*, 11119–11122.

[16] T. Murase, S. Sato, M. Fujita, *Angew. Chem. Int. Ed.* **2007**, *46*, 5133–5136; *Angew. Chem.* **2007**, *119*, 5225–5228.

[17] For recent examples of self-assembled cages with palladium(II) and pyridyl-based ligands, see a) M. Käseborn, J. J. Holstein, G. H. Clever, A. Lützen, *Angew. Chem. Int. Ed.* **2018**, *57*, 12171–12175; *Angew. Chem.* **2018**, *130*, 12349–12353; b) D. Preston, J. J. Sutton, K. C. Gordon, J. D. Crowley, *Angew. Chem. Int. Ed.* **2018**, *57*, 8659–8663; *Angew. Chem.* **2018**, *130*, 8795–8799; c) T. Tateishi, S. Takahashi, A. Okazawa, V. Martí-Centelles, J. Wang, T. Kojima, P. J. Lusby, H. Sato, S. Hiraoka, *J. Am. Chem. Soc.* **2019**, *141*, 19669–19676; d) T. Tsutsui, L. Catti, K. Yoza, M. Yoshizawa, *Chem. Sci.* **2020**, *11*, 8145–8150; e) S. Samantray, S. Krishnaswamy, D. K. Chand, *Nat. Commun.* **2020**, *11*, 880; f) J. E. M. Lewis, A. Tarzia, A. J. P. White, K. E. Jelfs, *Chem. Sci.* **2020**, *11*, 677–683; g) P. Howlader, S. Mondal, S. Ahmed, P. S. Mukherjee, *J. Am. Chem. Soc.* **2020**, *142*, 20968–20972; h) R. A. S. Vasdev, J. A. Findlay, D. R. Turner, J. D. Crowley, *Chem. Asian J.* **2021**, *16*, 39–43; i) R.-J. Li, F. Fadaei-Tirani, R. Scopelliti, K. Severin, *Chem. Eur. J.* **2021**, *27*, 9439–9445; j) L. S. Lisboa, D. Preston, C. J. McAdam, L. J. Wright, C. G. Hartinger, J. D. Crowley, *Angew. Chem. Int. Ed.* **2022**, *61*, e202201700; *Angew. Chem.* **2022**, *134*, e202201700.

[18] For relevant reviews of metallosupramolecular self-assembly with palladium(II), see a) D. Bardhan, D. K. Chand, *Chem. Eur. J.* **2019**, *25*, 12241–12269; b) S. Pullen, J. Tessarolo, G. H. Clever, *Chem. Sci.* **2021**, *12*, 7269–7293; c) A. J. McConnell, *Chem. Soc. Rev.* **2022**, *51*, 2957–2971.

[19] Metal complexes with photoswitchable ligand have been reviewed, see O. Galangau, L. Norel, S. Rigaut, *Dalton Trans.* **2021**, *50*, 17879–17891.

[20] a) M. Yamamura, Y. Okazaki, T. Nabeshima, *Chem. Commun.* **2012**, *48*, 5724–5726; b) M. Yamamura, K. Yamakawa, Y. Okazaki, T. Nabeshima, *Chem. Eur. J.* **2014**, *20*, 16258–16265; c) M. Lohse, K. Nowosinski, N. L. Traulsen, A. J. Achazi, L. K. S. von Krbek, B. Paulus, C. A. Schalley, S. Hecht, *Chem. Commun.* **2015**, *51*, 9777–9780; d) P. Cecot, A. Walczak, G. Markiewicz, A. R. Stefankiewicz, *Inorg. Chem. Front.* **2021**, *8*, 5195–5200.

[21] S. Fu, Q. Luo, M. Zang, J. Tian, Z. Zhang, M. Zeng, Y. Ji, J. Xu, J. Liu, *Mater. Chem. Front.* **2019**, *3*, 1238–1243.

[22] R. Sekiya, A. Díaz-Moscoso, P. Ballester, *Chem. Eur. J.* **2018**, *24*, 2182–2191.

[23] T. Sakano, T. Ohashi, M. Yamanaka, K. Kobayashi, *Org. Biomol. Chem.* **2015**, *13*, 8359–8364.

[24] a) D. A. McMorran, P. J. Steel, *Angew. Chem. Int. Ed.* **1998**, *37*, 3295–3297; *Angew. Chem.* **1998**, *110*, 3495–3497; b) P. J. Steel, D. A. McMorran, *Chem. Asian J.* **2019**, *14*, 1098–1101.

[25] a) R.-J. Li, J. J. Holstein, W. G. Hiller, J. Andréasson, G. H. Clever, *J. Am. Chem. Soc.* **2019**, *141*, 2097–2103; b) R.-J. Li, J. Tessarolo, H. Lee, G. H. Clever, *J. Am. Chem. Soc.* **2021**, *143*, 3865–3873; c) S. Juber, S. Wingbermühle, P. Nuernberger, G. H. Clever, L. V. Schäfer, *Phys. Chem. Chem. Phys.* **2021**, *23*, 7321–7332.

[26] C. Stuckhardt, D. Roke, W. Danowski, E. Otten, S. J. Wezenberg, B. L. Feringa, *Beilstein J. Org. Chem.* **2019**, *15*, 2767–2773.

[27] a) S.-S. Sun, J. A. Anspach, A. J. Lees, *Inorg. Chem.* **2002**, *41*, 1862–1869; b) S. Oldknow, D. R. Martir, V. E. Pritchard, M. A. Blitz, C. W. G. Fishwick, E. Zysman-Colman, M. J. Hardie, *Chem. Sci.* **2018**, *9*, 8150–8159; c) E. Britton, R. J. Ansell, M. J. Howard, M. J. Hardie, *Inorg. Chem.* **2021**, *60*, 12912–12923.

[28] H. Lee, J. Tessarolo, D. Langbehn, A. Baksi, R. Herges, G. H. Clever, *J. Am. Chem. Soc.* **2022**, *144*, 3099–3105.

[29] A. D. W. Kennedy, R. G. DiNardi, L. L. Fillbrook, W. A. Donald, J. E. Beves, *Chem. Eur. J.* **2022**, *28*, e202104461.

[30] a) D. Bléger, J. Schwarz, A. M. Brouwer, S. Hecht, *J. Am. Chem. Soc.* **2012**, *134*, 20597–20600; b) C. Knie, M. Utecht, F. Zhao, H. Kulla, S. Kovalenko, A. M. Brouwer, P. Saalfrank, S. Hecht, D. Bléger, *Chem. Eur. J.* **2014**, *20*, 16492–16501.

[31] Examples of applications using *ortho*-fluoroazobenzenes: For a gold(I) complex, see a) C. Cazorla, L. Casimiro, T. Arif, C. Deo, N. Goual, P. Retailleau, R. Métivier, J. Xie, A. Voituriez, A. Marinetti, N. Bogliotti, *Dalton Trans.* **2021**, *50*, 7284–7292. For examples in MOFs, see b) D. Hermann, H. A. Schwartz, M. Werker, D. Schaniel, U. Ruschewitz, *Chem. Eur. J.* **2019**, *25*, 3606–3616. For an example controlling zebra fish, see c) L. Albert, J. Nagpal, W. Steinchen, L. Zhang, L. Werel, N. Djokovic, D. Ruzic, M. Hoffarth, J. Xu, J. Kaspareit, F. Abendroth, A. Royant, G. Bange, K. Nikolic, S. Ryu, Y. Dou, L.-O. Essen, O. Vázquez, *ACS Cent. Sci.* **2022**, *8*, 57–66; d) A. Kerckhoffs, Z. Bo, S. E. Penty, F. Duarte, M. J. Langton, *Org. Biomol. Chem.* **2021**, *19*, 9058–9067. For examples as anion transporters, see e) A. Kerckhoffs, M. J. Langton, *Chem. Sci.* **2020**, *11*, 6325–6331; f) T. G. Johnson, A. Sadeghi-Kelishadi, M. J. Langton, *J. Am. Chem. Soc.* **2022**, *144*, 10455–10461. For an example controlling gene expression, see g) A. Paul, J. Huang, Y. Han, X. Yang, L. Vuković, P. Král, L. Zheng, A. Herrmann, *Chem. Sci.* **2021**, *12*, 2646–2654. For chaotic behavior in polymers, see h) K. Kumar, C. Knie, D. Bléger, M. A. Peletier, H. Friedrich, S. Hecht, D. J. Broer, M. G. Debije, A. P. H. J. Schenning, *Nat. Commun.* **2016**, *7*, 11975. For a liquid crystal example, see i) M. Saccone, K. Kuntze, Z. Ahmed, A. Siiskonen, M. Giese, A. Priimagi, *J. Mater. Chem. C* **2018**, *6*, 9958–9963. For examples in self-assembly, see j) H. Huang, T. Orlova, B. Matt, N. Katsonis, *Macromol. Rapid Commun.* **2018**, *39*, 1700387; k) T.-G. Zhan, M.-D. Lin, J. Wei, L.-J. Liu, M.-Y. Yun, L. Wu, S.-T. Zheng, H.-H. Yin, L.-C. Kong, K.-D. Zhang, *Polym. Chem.* **2017**, *8*, 7384–7389. For crystalline properties, see l) O. S. Bushuyev, A. Tomberg, J. R. Vinden, N. Moitessier, C. J. Barrett, T. Friščić, *Chem. Commun.* **2016**, *52*, 2103–2106; m) O. S. Bushuyev, A. Tomberg, T. Friščić, C. J. Barrett, *J. Am. Chem. Soc.* **2013**, *135*, 12556–12559; n) D. Hermann, H. A. Schwartz, U. Ruschewitz, *ChemistrySelect* **2017**, *2*, 11846–11852. For details of through-space ^{19}F-^{19}F coupling, see o) S. K. Rastogi, R. A. Rogers, J. Shi, C. T. Brown, C. Salinas, K. M. Martin, J. Armitage, C. Dorsey, G. Chun, P. Rinaldi, W. J. Brittain, *Magn. Reson. Chem.* **2016**, *54*, 126–131.

[32] Deposition numbers 2162330 (for photoswitch **1**), 2166455 (for $[Pd_2(E\text{-}\mathbf{1})_4](BF_4)_4$), and 2166449 (for $[Pd(Z\text{-}\mathbf{1})_2](BF_4)_2$) contain the supplementary crystallographic data for this paper. These data are provided free of charge by the joint Cambridge Crystallographic Data Centre and Fachinformationszentrum Karlsruhe Access Structures service.

[33] J. Harada, K. Ogawa, *Chem. Soc. Rev.* **2009**, *38*, 2244–2252.

[34] a) D. Samanta, J. Gemen, Z. Chu, Y. Diskin-Posner, L. J. W. Shimon, R. Klajn, *Proc. Natl. Acad. Sci. USA* **2018**, *115*, 9379–9384; b) D. Samanta, D. Galaktionova, J. Gemen, L. J. W. Shimon, Y. Diskin-Posner, L. Avram, P. Král, R. Klajn, *Nat. Commun.* **2018**, *9*, 641; c) J. Gemen, J. Ahrens, L. J. W. Shimon, R. Klajn, *J. Am. Chem. Soc.* **2020**, *142*, 17721–17729; d) M. Canton, A. B. Grommet, L. Pesce, J. Gemen, S. Li, Y. Diskin-Posner, A. Credi, G. M. Pavan, J. Andréasson, R. Klajn, *J. Am. Chem. Soc.* **2020**, *142*, 14557–14565; e) L. Pesce, C. Perego, A. B. Grommet, R. Klajn, G. M. Pavan, *J. Am. Chem. Soc.* **2020**, *142*, 9792–9802; f) A. B. Grommet, M. Feller, R. Klajn, *Nat. Nanotechnol.* **2020**, *15*, 256–271.

[35] J. E. M. Lewis, E. L. Gavey, S. A. Cameron, J. D. Crowley, *Chem. Sci.* **2012**, *3*, 778–784.

[36] The difference after adding DMAP (*Z*-**1**: 95 % to 89 %) is likely due to *E*-**1** forming undefined oligomeric species, which are not observed in the ^1H NMR spectrum.

[37] a) S. Lv, X. Li, L. Yang, X. Wang, J. Zhang, G. Zhang, J. Jiang, *J. Phys. Chem. A* **2020**, *124*, 9692–9697; b) T. Bartelmann, F. Gnannt, M. Zitzmann, P. Mayer, H. Dube, *Chem. Sci.* **2021**, *12*, 3651–3659.

[38] S. Shinkai, T. Nakaji, T. Ogawa, K. Shigematsu, O. Manabe, *J. Am. Chem. Soc.* **1981**, *103*, 111–115.

[39] E. Busseron, J. Lux, M. Degardin, J. Rebek, *Chem. Commun.* **2013**, *49*, 4842–4844.

[40] K. Dąbrowa, P. Niedbała, J. Jurczak, *Chem. Commun.* **2014**, *50*, 15748–15751.

[41] a) A. A. Beharry, O. Sadovski, G. A. Woolley, *J. Am. Chem. Soc.* **2011**, *133*, 19684–19687; b) M. Dong, A. Babalhavaeji, S. Samanta, A. A. Beharry, G. A. Woolley, *Acc. Chem. Res.* **2015**, *48*, 2662–2670.

[42] A. D. W. Kennedy, I. Sandler, J. Andréasson, J. Ho, J. E. Beves, *Chem. Eur. J.* **2020**, *26*, 1103–1110.

[43] a) R. S. L. Gibson, J. Calbo, M. J. Fuchter, *ChemPhotoChem* **2019**, *3*, 372–377; b) J. L. Greenfield, M. A. Gerkman, R. S. L. Gibson, G. G. D. Han, M. J. Fuchter, *J. Am. Chem. Soc.* **2021**, *143*, 15250–15257.

[44] R. Vulcano, P. Pengo, S. Velari, J. Wouters, A. De Vita, P. Tecilla, D. Bonifazi, *J. Am. Chem. Soc.* **2017**, *139*, 18271–18280.

[45] J. Garcia-Amorós, M. C. R. Castro, S. Nonell, S. Vílchez, J. Esquena, M. M. M. Raposo, D. Velasco, *J. Phys. Chem. C* **2019**, *123*, 23140–23144.

[46] D. P. August, G. S. Nichol, P. J. Lusby, *Angew. Chem. Int. Ed.* **2016**, *55*, 15022–15026; *Angew. Chem.* **2016**, *128*, 15246–15250.

[47] Other references that use the same guests, e.g. Ref 23 and a) G. H. Clever, S. Tashiro, M. Shionoya, *J. Am. Chem. Soc.* **2010**, *132*, 9973–9975; b) S. Ganta, D. K. Chand, *Inorg. Chem.* **2018**, *57*, 3634–3645; c) D. Preston, J. E. M. Lewis, J. D. Crowley, *J. Am. Chem. Soc.* **2017**, *139*, 2379–2386, and; d) D. Preston, K. M. Patil, A. T. O'Neil, R. A. S. Vasdev, J. A. Kitchen, P. E. Kruger, *Inorg. Chem. Front.* **2020**, *7*, 2990–3001.

[48] a) P. Thordarson, *Chem. Soc. Rev.* **2011**, *40*, 1305–1323; b) D. Brynn Hibbert, P. Thordarson, *Chem. Commun.* **2016**, *52*, 12792–2805; c) http://supramolecular.org.

[49] a) V. Martí-Centelles, A. L. Lawrence, P. J. Lusby, *J. Am. Chem. Soc.* **2018**, *140*, 2862–2868; b) R. L. Spicer, A. D. Stergiou, T. A. Young, F. Duarte, M. D. Symes, P. J. Lusby, *J. Am. Chem. Soc.* **2020**, *142*, 2134–2139; c) J. Wang, T. A. Young, F. Duarte, P. J. Lusby, *J. Am. Chem. Soc.* **2020**, *142*, 17743–17750.

Manuscript received: April 19, 2022
Version of record online: August 16, 2022